

# Highly Efficient Pyridylpyrazole Ligands for the Heck Reaction. A Combined Experimental and Computational Study

Vanessa Montoya,<sup>†</sup> Josefina Pons,<sup>\*,†</sup> Vicenç Branchadell,<sup>\*,‡</sup> Jordi Garcia-Antón,<sup>†</sup>  
Xavier Solans,<sup>§,⊥</sup> Mercè Font-Bardía,<sup>§</sup> and Josep Ros<sup>†</sup>

Departament de Química, Unitat de Química Inorgànica, Universitat Autònoma de Barcelona, 08193-Bellaterra, Barcelona, Spain, Departament de Química, Unitat de Química Física, Universitat Autònoma de Barcelona, 08193-Bellaterra, Barcelona, Spain, and Cristal·lografia, Mineralogia i Dipòsits Minerals, Universitat de Barcelona, Martí i Franquès s/n, 08028-Barcelona, Spain

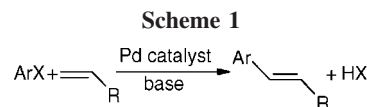
Received September 14, 2007

Several [PdCl<sub>2</sub>(L)] complexes, where L is a pyridylpyrazole ligand, have been used as precatalysts in the Heck reactions between phenyl halides and *tert*-butyl acrylate. The used ligands differ from each other in the substitution at N1. The best results are obtained when this substituent is a hydroxyethyl group, and the corresponding complexes yield good results even for the reaction of chlorobenzene. Theoretical studies have shown that the presence of an OH group in the N1 substituent favors Pd–X dissociation, since it stabilizes the resulting cationic complex and the dissociation becomes thermodynamically favorable even in the absence of a coordinating solvent molecule.

## Introduction

The Heck reaction is one of the most widely used palladium-catalyzed reactions in organic synthesis.<sup>1–3</sup> The reaction consists in the vinylation of aryl halides, and it was first reported by Mizoroki and Heck in the early 1970s<sup>4</sup> (Scheme 1). In the following decades, the chemical community has searched for active and stable palladium catalysts, which should be versatile and efficient.<sup>5–9</sup>

For several years, aryl bromides and iodides were preferably used as substrates in such reactions, because aryl chlorides are transformed very sluggishly by standard palladium catalysts, due to the strength of the C–Cl bond. There has been a growing interest in finding catalytic systems that can successfully catalyze cross-coupling reactions with aryl chlorides,<sup>10</sup> since they are widely available, industrially important, and generally less expensive than their bromide and iodide counterparts. In the past few years, important advances have been done in this direction, with part of this success owed to the development of new palladium complexes that contain electron-rich and bulky



ligands (namely, phosphines, carbenes, and N-heterocycles)<sup>11</sup> that improve their catalytic activity in coupling reactions.

The most studied reaction is normally carried out in the presence of phosphine ligands and a base under an inert atmosphere. However, phosphine ligands are expensive, toxic, and unrecoverable. For this reason, much interest has been devoted to the search for new phosphine-free Pd catalysts. In particular, N,N-ligands have been shown to yield high-turnover-number palladium catalysts in simple Heck reactions.<sup>11</sup>

The Heck reaction has also been the subject of theoretical studies.<sup>12–23</sup> Different kinds of ligands have been considered. In particular, Albert et al.<sup>12</sup> have studied the reaction between ethylene and bromobenzene catalyzed by a palladium complex coordinated to model diaminocarbene ligands. On the other hand, Deeth et al.<sup>13,14,21</sup> have studied several steps of the reaction

\* Corresponding authors. Fax: 34-93 581 31 01. E-mail: Josefina.Pons@uab.es.

<sup>†</sup> Unitat de Química Inorgànica, Universitat Autònoma de Barcelona.

<sup>‡</sup> Unitat de Química Física, Universitat Autònoma de Barcelona.

<sup>§</sup> Cristal·lografia, Mineralogia i Dipòsits Minerals, Universitat de Barcelona.

<sup>⊥</sup> Deceased September 3, 2007, during the preparation of the manuscript.

(1) Heck, R. F. *Palladium Reagents in Organic Synthesis*; Academic Press: London, UK, 1985.

(2) Heck, R. F. *Pure Appl. Chem.* **1978**, *50*, 691.

(3) Heck, R. F. *Acc. Chem. Res.* **1979**, *12*, 146.

(4) Heck, R. F.; Nolley, J. P. *J. Org. Chem.* **1972**, *37*, 2320.

(5) Bedford, R. B.; Cazin, C. S. J.; Holder, D. *Coord. Chem. Rev.* **2004**, *248*, 2283.

(6) Heck, R. F. In *Comprehensive Organic Synthesis*; Trost, B. M., Fleming, I., Eds.; Pergamon Press: Oxford, 1991; Vol 4.

(7) De Meijere, A.; Braese, S. In *Transition Metal Catalyzed Reactions*; Davies, S. G., Murahashi, S. I., Eds.; Blackwell Science: Oxford, UK, 1999.

(8) Shibasaki, M.; Boden, C. D. J.; Kojima, A. *Tetrahedron* **1997**, *53*, 7371.

(9) Beletskaya, I. P.; Cheprakov, A. V. *Chem. Rev.* **2000**, *100*, 3009.

(10) Herrmann, W. A.; Ofele, K.; von Preysing, D.; Schneider, S. K. *J. Organomet. Chem.* **2003**, *687*, 229.

(11) Farina, V. *Adv. Synth. Catal.* **2004**, *346*, 1553.

(12) Albert, K.; Gisdakis, P.; Rösch, N. *Organometallics* **1998**, *17*, 1608.

(13) Deeth, R. J.; Smith, A.; Hii, K. K.; Brown, J. M. *Tetrahedron Lett.* **1999**, *39*, 3229.

(14) Hii, K. K.; Claridge, T. D. W.; Brown, J. M.; Smith, A.; Deeth, R. J. *Helv. Chim. Acta* **2001**, *84*, 3043.

(15) von Schenck, H.; Strömberg, S.; Zetterberg, K.; Ludwig, M.; Åkermark, B.; Svensson, M. *Organometallics* **2001**, *20*, 2813.

(16) Sundermann, A.; Uzan, O.; Martin, J. M. L. *Chem.–Eur. J.* **2001**, *7*, 1703.

(17) von Schenck, H.; Åkermark, B.; Svensson, M. *Organometallics* **2002**, *21*, 2248.

(18) von Schenck, H.; Åkermark, B.; Svensson, M. *J. Am. Chem. Soc.* **2003**, *125*, 3503.

(19) Lin, B. L.; Liu, L.; Fu, Y.; Luo, S. W.; Chen, Q.; Guo, Q. X. *Organometallics* **2004**, *23*, 2114.

(20) Balcells, D.; Maseras, F.; Keay, B. A.; Ziegler, T. *Organometallics* **2004**, *23*, 2784.

(21) Deeth, R. J.; Smith, A.; Brown, J. M. *J. Am. Chem. Soc.* **2004**, *126*, 7144.

(22) Datta, G. K.; von Schlenk, H.; Hallberg, A.; Larhed, M. *J. Org. Chem.* **2006**, *71*, 3896.

(23) Lee, M. T.; Lee, H. M.; Hu, C. H. *Organometallics* **2007**, *26*, 1317.

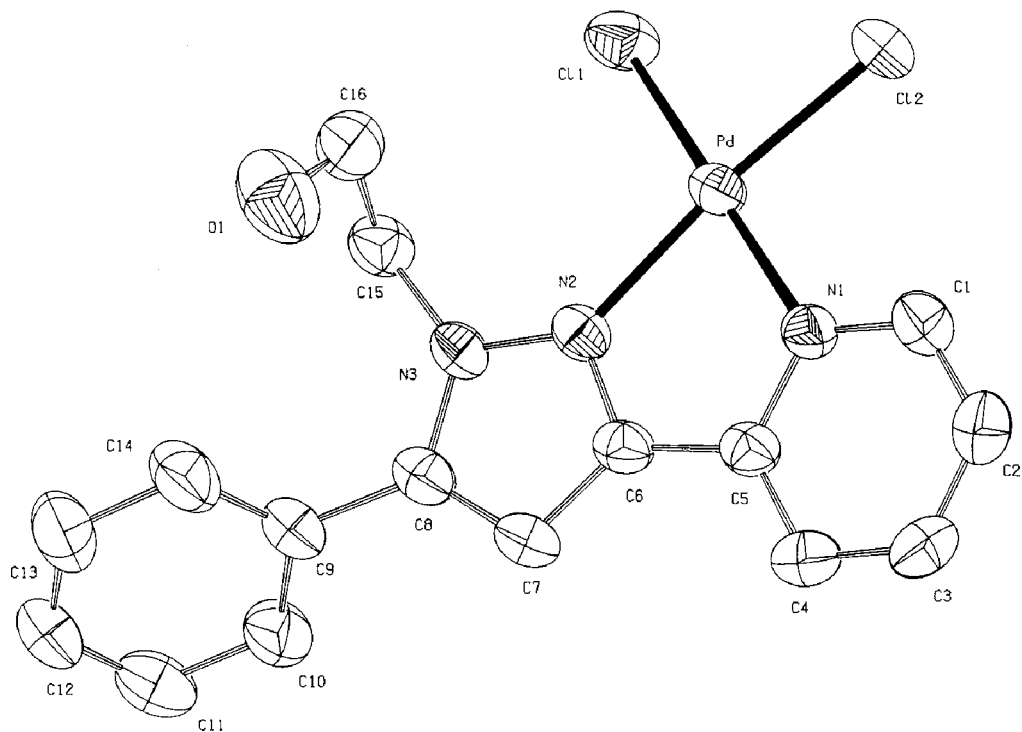


**Figure 1.** ORTEP drawing of complex **2a** (ellipsoids are shown at the 50% probability level).

using a model diphosphino ligand. A similar kind of ligand has been used by Sundermann et al.<sup>16</sup> in the study of the complete reaction path for the reaction between iodobenzene and ethylene. Finally, von Schlenck et al.<sup>15,17</sup> have studied the olefin insertion step in several (diimine)Pd(II) cationic complexes.

Recently, the synthesis and characterization of several pyridylpyrazole-derived ligands with different substitutions in the 3,5- position<sup>24–27</sup> has been reported in the literature, and the reactivity of some of these ligands with Pd(II) has been studied in our laboratory.<sup>26,28</sup> A common problem in the coordination chemistry of pyridylpyrazole ligands to metal ions is the low solubility of these complexes in organic solvents, mainly caused by  $\pi$ - $\pi$  stacking interactions. This solubility can be increased by incorporating an alkyl or hydroxyalkyl group at the N1-position of the pyrazole ring. In recent papers, we have reported the synthesis and characterization of several *N*-alkyl-3,5-pyrazole-derived ligands with ethyl, octyl,<sup>29</sup> and hydroxyethyl groups at the N1-position.<sup>26</sup> We have also studied their reactivity toward Pd(II).<sup>28,30</sup> Very recently, we have shown that cationic pyridylpyrazole allylpalladium  $[\text{Pd}(\eta^3\text{-C}_3\text{H}_5)(\text{L})](\text{BF}_4)$  complexes undertake an apparent allyl rotation in solution.<sup>31</sup> This process presents low  $\Delta G^\ddagger$  values and is favored by coordinating solvents or traces of water present in the solvent. This process was also observed in a noncoordinating solvent such as

dichloromethane with the ligand (2-(5-phenyl-3-pyridin-2-yl-pyrazol-1-yl)ethanol), which contained a hydroxyethyl group at the N1-position. In this case, the process would take place through an intramolecular associative mechanism, which implies a hemilabile coordination of the OH to the metal.

In a continuation of our investigations we describe in this paper the study of the catalytic activity of  $[\text{PdCl}_2(\text{L})]$  complexes with pyridylpyrazole (L) ligands in the Heck reaction of vinylation of aryl halides with the main objective of checking the influence of the hydroxyethyl fragment in this reaction. Most of the studied complexes are active catalysts, and some of them have shown a remarkable versatility, being very active with aryl chlorides. Experimental results have been rationalized through theoretical calculations.

## Results and Discussion

**Synthesis and Characterization of Complex 2a.** The ligand **1a** (see Figure 2) was prepared in good yields using the method described in the literature.<sup>31</sup> The reaction of  $[\text{PdCl}_2(\text{CH}_3\text{CN})_2]$  with **1a** in acetonitrile at room temperature gives the new palladium(II) complex **2a** as orange crystals in quantitative yield. Complex **2a** has been fully characterized by elemental analysis, conductivity measurements, IR, and <sup>1</sup>H NMR and <sup>13</sup>C{<sup>1</sup>H} NMR spectroscopies. Moreover, its structure was confirmed by X-ray crystallography (see Figure 1 and the Supporting Information). The crystal structure of complex **2a** is similar to that of related complexes found in the literature.<sup>26,28,30</sup>

**Heck Reactions Using Pd(II) Complexes with Pyridylpyrazole Ligands 1.** Complex **2a** and other  $[\text{PdCl}_2\text{L}]$  complexes (**2**) containing different pyridylpyrazole ligands<sup>26,28,30</sup> (**1**) (see Figure 2) have been used as precatalysts in the Heck reaction between phenyl halides and *tert*-butyl acrylate. In some cases, the reaction has also been studied using styrene as olefin.

The reaction progress was analyzed by GLC. In all cases, the reactions led to the formation of *trans* compound exclusively (<sup>1</sup>H NMR). The results obtained are summarized in Table 1.

(24) Casabó, J.; Pons, J.; Siddiqi, K. S.; Teixidor, F.; Molins, E.; Miravittles, C. *J. Chem. Soc., Dalton Trans.* **1989**, 1401.

(25) Chadghan, A.; Pons, J.; Caubet, A.; Casabó, J.; Ros, J.; Alvarez-Larena, A.; Piniella, J. F. *Polyhedron* **2000**, *19*, 855.

(26) Perez, J. A.; Pons, J.; Solans, X.; Font-Bardia, M.; Ros, J. *Inorg. Chim. Acta* **2005**, *358*, 617.

(27) Thiel, W. R.; Eppinger, J. *Chem.—Eur. J.* **1997**, *3*, 696.

(28) Montoya, V.; Pons, J.; Garcia-Antón, J.; Solans, X.; Font-Bardia, M.; Ros, J. *Inorg. Chim. Acta* **2007**, *360*, 625.

(29) Montoya, V.; Pons, J.; Branchadell, V.; Ros, J. *Tetrahedron*, **2005**, *61*, 12377.

(30) Montoya, V.; Pons, J.; Solans, X.; Font-Bardia, M.; Ros, J. *Inorg. Chim. Acta* **2006**, *359*, 25.

(31) Montoya, V.; Pons, J.; Garcia-Antón, J.; Solans, X.; Font-Bardia, M.; Ros, J. *Organometallics* **2007**, *26*, 3183.

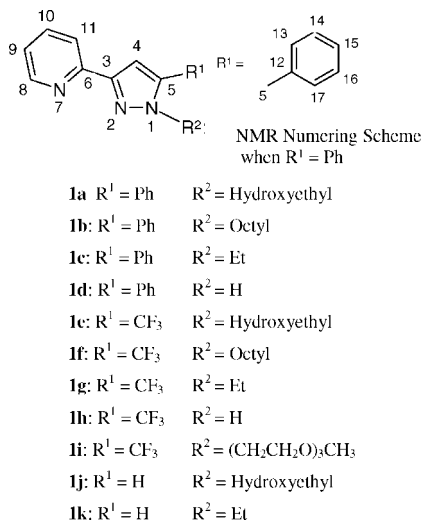


**Figure 2.** Pyridylpyrazole-derived ligands and NMR numbering scheme. **1k** and **1j** are the models used in theoretical calculations.

Preliminary catalytic studies of complex **2b** (0.1%) in a Heck reaction between bromobenzene and *tert*-butyl acrylate at 100 °C with NEt<sub>3</sub> as base and solvent showed that the reaction did not take place, so we decided to change the conditions using the same reagents but DMF as solvent at 140 °C and NBu<sub>4</sub>Br as additive. Under these conditions, a yield of 66% is obtained in 78 h, with a turnover number (TON) of 671 (entry 6).

During the reaction, a black solid precipitated from the reaction mixture. This solid was identified as Pd(0) through the mercury poisoning test.<sup>32</sup>

In order to study the influence of the alkylic chain in N1, we performed the reaction of phenyl bromide with *tert*-butyl acrylate in the presence of complex **2c**, which contains a shorter R<sup>2</sup> chain than **2b**. In this case, an increase in efficiency was observed (entry 8). We also tested a ligand without N1 substitution (**1d**), observing a major conversion in a shorter time (entry 10). The same reaction was also studied by changing the solvent from DMF to H<sub>2</sub>O. In this case, the efficiency decreases probably due to the low solubility of complex **2d** in water (entry 11).

To study the influence of the substituent in the 5-position, we carried out the Heck reaction with complexes containing an electron-withdrawing group such as CF<sub>3</sub> (ligands **1f**, **1g**, and **1h**). For complexes **2f** and **2g** the conversion was similar to or lower than that for analogous complexes (**2b** and **2c**, respectively) in the same conditions (entries 17 and 18). In contrast, for complex **2h** (entry 20) a low conversion is observed, probably because in solution this complex is not neutral since the base (NEt<sub>3</sub>) can extract the N–H acidic proton of the pyrazolic ligand, producing an ionic complex with different properties.

Moreover, to study the influence of the nature of the N1-substituent, we have performed the reaction with complexes containing a N1 hydroxyethyl substituent (complexes **2a** and **2e**). Surprisingly, in these cases we obtained the best results (entries 1 and 13), better than results reported in the literature with a similar catalyst.<sup>33</sup> In order to know if these excellent results were due to a possible hydrogen bond interaction between

the hydroxyethyl substituent of the complexes and *tert*-butyl acrylate, we performed the reaction with **2a** and **2e** using styrene as olefin (entries 4 and 15). With this substrate a minor conversion was observed attributable to the different electron-withdrawing character of the substituent (phenyl). The decrease of conversion is similar to that observed for **2g** (entries 18 and 19), where the ligand does not contain any oxygen atom. So, the possible hydrogen bond interaction with *tert*-butyl acrylate does not seem to play any role.

In order to establish if the high conversion observed for **2a** and **2e** is due to the hydroxyethyl substituent or only to the oxygen atom, we studied the reaction with complex **2i**, which contains a N1 polyether. The conversion for the reaction of bromobenzene (entry 23) is similar to that obtained for **2f** (entry 17), where the R<sup>2</sup> has a similar length but does not contain any oxygen atom.

The efficiency of the reaction depends on the aryl halide, and the best results are obtained, as expected, for iodobenzene (entries 2, 14, and 22). However, for the reaction of chlorobenzene a good conversion is obtained with complexes **2a** and **2e** in a long reaction time (entries 5 and 16). These results are excellent when compared with the available literature<sup>33</sup> and confirm the potentialities of pyridylpyrazole ligands in the Heck reaction.

Finally, to optimize the process, we have utilized a lower proportion of catalysts to increase the TON. Similar conversions are obtained when reducing the precatalyst concentration from 0.1 to 0.01% in most cases (entries 3, 7, and 12), whereas a slight decrease is observed for **1h** (entries 20 and 21).

**Theoretical Calculations.** In order to understand the role of the R<sup>2</sup> group in the Heck reactions, we have studied the reaction between iodobenzene and methyl acrylate (MA) catalyzed by Pd(0) complexes bearing model ligands **1j** (**3j**) and **1k** (**3k**) (see Figure 2). Acetonitrile has been used as solvent since its dielectrical constant is similar to that of DMF used in experiments. The complete reaction mechanism is summarized in Scheme 2.

The catalytic cycle begins with the oxidative addition of PhI to the Pd(0) complex **3**. This process takes place in two steps. In the first one, iodobenzene coordinates to the Pd atom of **3** to form a η<sup>2</sup>-CC complex without energy barrier. The second step involves the cleavage of the C–I bond and the formation of the Pd(II) complex **4**. The most stable isomers of **4j** and **4k** are the ones in which the iodide ligand is *cis* with respect to the pyrazole ring. The alternative *trans* isomers are 1.3 (**4j**) and 1.5 (**4k**) kcal mol<sup>-1</sup> higher in energy at the B3LYP/LANL2DZ(d) level of calculation.

Table 2 presents the Gibbs reaction and activation energies computed for the addition of PhI to **3j** and **3k**. For comparison, we have also considered the addition of bromobenzene and chlorobenzene to **3j**. Figure 3 shows the structures of the stationary points corresponding to the oxidative addition of PhI to **3j**.

As we can observe, the two Pd–N distances in **3j** differ from each other by 0.6 Å, the Pd–N(pyrazole) distance being the shortest one. A more symmetrical structure (**3'j**) has also been obtained with an energy only 0.03 kcal mol<sup>-1</sup> higher than **3j** at the B3LYP/LANL2DZ(d) level of calculation. However, it becomes less favored in terms of Gibbs energy both in the gas phase (1.0 kcal mol<sup>-1</sup>) and in solution (3.3 kcal mol<sup>-1</sup>). We have also obtained an additional structure, **3''j**, in which the ligand is also coordinated through the OH group, but it is 2.8 kcal mol<sup>-1</sup> higher in energy than **3j** at the B3LYP/LANL2DZ(d) level.

(32) Widegren, J. A.; Finke, R. G. *J. Mol. Catal. A: Chem.* **2003**, *198*, 317.

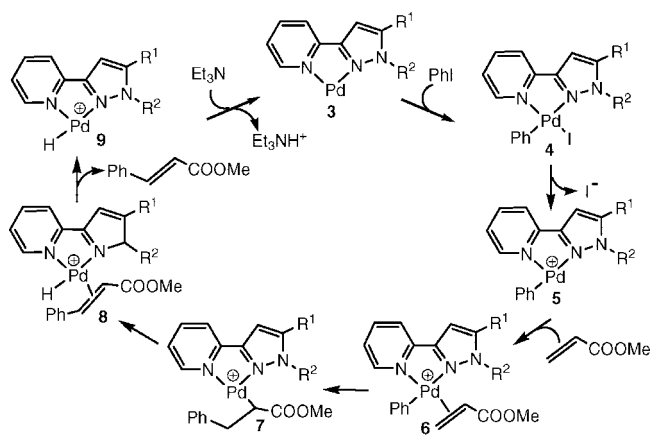
(33) Najera, C.; Gil-Moltó, J.; Karlström, S.; Falvello, L. R. *Org. Lett.* **2003**, *5*, 1451.

Table 1. Heck Coupling Reaction<sup>a</sup> between Phenyl Halides and *tert*-Butyl Acrylate<sup>b</sup> in the Presence of PdCl<sub>2</sub>L Precatalysts

entry	halide	L <sup>c</sup>	% precatalyst	solvent	T (°C)	t (h)	% yield <sup>d</sup>	TON	TOF
1	Br	<b>1a</b>	0.1	DMF	140	2	98	1080	540
2	I	<b>1a</b>	0.1	DMF	140	1	100	1101	1101
3	I	<b>1a</b>	0.01	DMF	140	1	100	11016	11016
4 <sup>e</sup>	I	<b>1a</b>	0.01	DMF	140	5	91	10024	2004
5	Cl	<b>1a</b>	0.01	DMF	140	51	97	10687	209
6	Br	<b>1b</b>	0.1	DMF	140	78	66	671	8.6
7	Br	<b>1b</b>	0.01	DMF	140	72	67	6816	94.8
8	Br	<b>1c</b>	0.1	DMF	140	30	84	891	29.7
9	Cl	<b>1c</b>	0.1	DMF	140	44	11	116	2.6
10	Br	<b>1d</b>	0.1	DMF	140	14	96	1056	75.4
11	Br	<b>1d</b>	0.1	H <sub>2</sub> O	100	30	5	54	1.8
12	Br	<b>1d</b>	0.01	DMF	140	20	90	991	49.5
13	Br	<b>1e</b>	0.1	DMF	140	1	93	1005	1005
14	I	<b>1e</b>	0.1	DMF	140	1	96	1038	1038
15 <sup>e</sup>	I	<b>1e</b>	0.01	DMF	140	6	87	9583	1597
16	Cl	<b>1e</b>	0.01	DMF	140	59	89	9804	166
17	Br	<b>1f</b>	0.01	DMF	140	47	54	584	12.4
18	Br	<b>1g</b>	0.1	DMF	140	4	87	874	218
19 <sup>e</sup>	Br	<b>1g</b>	0.01	DMF	140	10	78	8127	812
20	Br	<b>1h</b>	0.1	DMF	140	23	63	627	27.3
21	Br	<b>1h</b>	0.01	DMF	140	27	51	496	18.4
22	I	<b>1i</b>	0.01	DMF	140	14	100	11300	807
23	Br	<b>1i</b>	0.01	DMF	140	36	52	5626	156
24	Cl	<b>1i</b>	0.01	DMF	140	77	10	1081	14

<sup>a</sup> Reactions conditions: 1.0 equiv of phenyl halide, 1.5 equiv of alkene, 1.4 equiv of NEt<sub>3</sub>, 0.5 equiv of NBu<sub>4</sub>Br, 2 mL of solvent. <sup>b</sup> Except as otherwise indicated. <sup>c</sup> See Figure 2. <sup>d</sup> Determined by GC, based on the phenyl halide using decane as internal standard. <sup>e</sup> Styrene was used as olefin instead of *tert*-butyl acrylate.

Scheme 2

Table 2. Gibbs Activation and Reaction Energies<sup>a</sup> for the Oxidative Addition of PhX to **3**

	R <sup>2</sup> = CH <sub>2</sub> CH <sub>2</sub> OH		R <sup>2</sup> = Et	
	ΔG <sup>‡</sup>	ΔG <sup>°</sup>	ΔG <sup>‡</sup>	ΔG <sup>°</sup>
<b>3</b> + PhI → <b>3-PhI</b>		-5.0		-12.7
<b>3-PhI</b> → <b>4</b>	4.2	-36.6	3.3	-36.1
<b>3</b> + PhBr → <b>3-PhBr</b>		-4.2		
<b>3-PhBr</b> → <b>4<sub>Br</sub></b>	6.5	-38.2		
<b>3</b> + PhCl → <b>3-PhCl</b>		-4.1		
<b>3-PhCl</b> → <b>4<sub>Cl</sub></b>	8.5	-35.2		

<sup>a</sup> In acetonitrile solution at 298.15 K and 1 mol L<sup>-1</sup>. All values in kcal mol<sup>-1</sup>.

The oxidative addition of PhI is kinetically and thermodynamically very favorable for both **3j** and **3k**. The transition states corresponding to C–I cleavage are below the **3** + PhI asymptotes by -0.8 (**3j**) and -9.4 (**3k**) kcal mol<sup>-1</sup> in acetonitrile and by -10.5 (**3j**) and -11.3 (**3k**) kcal mol<sup>-1</sup> in the gas phase. The latter results can be compared with those reported by Sundermann et al.<sup>15</sup> for the addition of PhI to (diphosphinoethane)Pd, in which the transition state was 2.0 kcal mol<sup>-1</sup> above the reactants. These results show that pyridylpyrazole

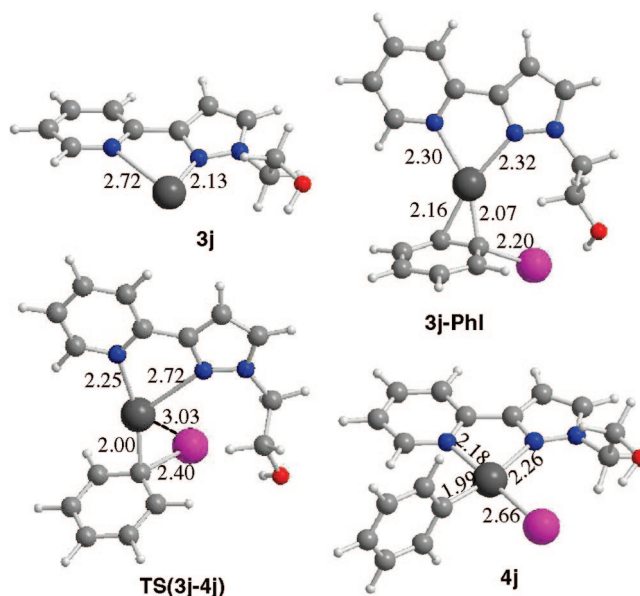
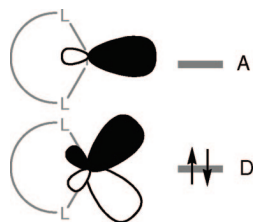


Figure 3. Structures of stationary points corresponding to the reaction between **3j** and phenyl iodide. Selected interatomic distances are in Å.

ligands are more efficient than diphosphino ligands in the activation of aryl halides.

Table 2 shows that **3j** may also be efficient in the activation of bromobenzene and chlorobenzene, since the corresponding transition states lie only 2.3 (PhBr) and 4.4 (PhCl) kcal mol<sup>-1</sup> above the reactants. The results corresponding to the addition of PhBr may be compared with those reported by Lee et al.,<sup>23</sup> which place the transition state about 25 kcal mol<sup>-1</sup> above the reactants using either nonchelate N-heterocyclic carbene or phosphine ligands.

The oxidative addition of the phenyl halide is accepted to be the rate-determining step of the overall process. For this reason it is interesting to compare the effect of different chelate ligands. Figure 4 shows the molecular orbitals of a chelate Pd(0)



**Figure 4.** Schematic representation of donor (D) and acceptor (A) molecular orbitals of a chelate PdL<sub>2</sub> complex.

**Table 3.** Energies<sup>a</sup> of Donor and Acceptor Molecular Orbitals<sup>b</sup> of Several Chelate Pd(0) Complexes

ligand <sup>c</sup>	D	A
<b>1a</b>	-0.13643	-0.03807
<b>1e</b>	-0.14491	-0.03986
<b>1j</b>	-0.13738	-0.03793
<b>1k</b>	-0.12557	-0.02827
dpe	-0.17072	-0.02585
dppe	-0.15620	-0.03225
dmmdiy	-0.11846	0.00625

<sup>a</sup> In a.u. <sup>b</sup> See Figure 4. <sup>c</sup> See Figure 2 for ligands **1**. dpe = 1,2-diphosphinoethane, dppe = 1,2-bis(diphenylphosphino)ethane, dmmdiy = 3,3'-dimethyl-1,1'-methylenediimidazol-2,2'-diylidene.

**Table 4.** Gibbs Reaction Energies<sup>a</sup> for Dissociation of Pd–Ligand Bonds in **4j** and **4k**

	<b>4j</b>	<b>4k</b>
Pd–I	-2.5	12.0
Pd–N(pyrazole)	7.9	11.4
Pd–N(pyridine)	13.8	19.9

<sup>a</sup> In acetonitrile solution at 298.15 K and 1 mol L<sup>-1</sup>. All values in kcal mol<sup>-1</sup>.

complex, which intervene in the interaction with the incoming aryl halide. The energies of these two orbitals have been computed for several PdL complexes, including the model ligands **1j** and **1k** and the experimentally used ligands **1a** and **1e** (see Table 3). We have also included two diphosphine and one dicarbene complexes. The interaction between Pd and the aryl halide molecule at the oxidative addition transition state is mainly due to the charge transfer from the donor orbital D to the  $\sigma^*_{C-X}$  orbital of PhX.

We can observe that complexes with pyridylpyrazole ligands **1** are better electron donors than diphosphino complexes. However, none of them reach the donor ability of the (dmmdiy)Pd complex. On the other hand, the complex with the model ligand **1j** has similar donor ability than the complex with **1a**. The relative donor abilities of complexes with **1a** and **1e** are in good agreement with their experimentally observed catalytic activities (see Table 1).

After oxidative addition, the next step in the mechanism involves the coordination of the alkene molecule, so that a vacant coordination site has to be created in **4**. There are two different ways for such a process: dissociation of the Pd–I bond, to form a cationic complex **5**, or dissociation of one of the Pd–N bonds. Table 4 shows the Gibbs reaction energies for such processes.

For **4j** the Pd–I dissociation is much more favorable than Pd–N dissociation, so that the formation of the **5j** cationic complex is expected to be favored and the reaction to proceed through a cationic catalytic cycle. **5j** is stabilized through the coordination of the oxygen atom of the hydroxyethyl group.

This stabilization is not possible in **5k** due to the absence of a hydroxyl group. For this reason, the dissociation of the Pd–I bond is not favorable. As a consequence, the dissociation of

**Table 5.** Gibbs Activation and Reaction Energies<sup>a</sup> for the Reaction between **5** and Methyl Acrylate (MA)

	R <sup>2</sup> = CH <sub>2</sub> CH <sub>2</sub> OH		R <sup>2</sup> = Et	
	$\Delta G^\ddagger$	$\Delta G^\circ$	$\Delta G^\ddagger$	$\Delta G^\circ$
<b>5</b> -MeCN $\rightarrow$ <b>5</b> + MeCN		2.0		14.3
<b>5</b> + MA $\rightarrow$ <b>6</b>	29.2	16.9	15.1	-1.1
<b>6</b> $\rightarrow$ <b>7</b>	5.8	-12.5	10.3	-6.8
<b>7</b> $\rightarrow$ <b>7'</b>	9.0	-3.3	8.6	-3.7
<b>7'</b> $\rightarrow$ <b>8</b>	3.0	2.9	2.6	1.8
<b>8</b> $\rightarrow$ <b>9</b> + MC <sup>b</sup>	15.6	-14.1	14.2	-4.9
<b>9</b> + Me <sub>3</sub> N $\rightarrow$ <b>3</b> + Me <sub>3</sub> NH <sup>+</sup>		15.0		12.3
<b>9</b> + Et <sub>3</sub> N $\rightarrow$ <b>3</b> + Et <sub>3</sub> NH <sup>+</sup>		14.0		11.4

<sup>a</sup> In acetonitrile solution at 298.15 K and 1 mol L<sup>-1</sup>. All values in kcal mol<sup>-1</sup>. <sup>b</sup> Methyl cinnamate.

the Pd–N(pyrazole) bond becomes slightly favored. In this case, the cationic mechanism may be in competition with a neutral mechanism.

The vacant coordination site created after Pd–I dissociation in **4k** may be occupied by a solvent molecule. We have studied the coordination of an acetonitrile molecule in **5k**, and the computed Gibbs reaction energy is -14.3 kcal mol<sup>-1</sup>. So, the dissociation of the Pd–I bond in **3k** assisted by a solvent molecule is thermodynamically favorable ( $\Delta G^\circ = -2.0$  kcal mol<sup>-1</sup>), and the cationic mechanism is also expected to be operative for **4k**. Regarding the coordination of acetonitrile to **5j**, the process is also favorable, but the corresponding Gibbs reaction energy is only -2.0 kcal mol<sup>-1</sup>.

We have studied the cationic catalytic cycle for both **5j** and **5k**. The corresponding Gibbs activation and reaction energies are presented in Table 5, while the structures of the stationary points corresponding to the reaction of **4j** are shown in Figures 5 and 6. In both cases we have considered as a previous step the dissociation of a coordinated solvent molecule in **5**.

The next step in the reaction mechanism is the coordination of methyl acrylate (MA). The most stable conformer of free methyl acrylate presents an *s-cis* arrangement of the carbonyl with respect to the C=C bond. However, in complexes **6j** and **6k** an *s-trans* arrangement is preferred, especially for **6j** due to a hydrogen bond stabilization.

Methyl acrylate coordinates to **5** to form an  $\eta^1$ -O complex. The Gibbs formation energies of the complexes with **5j** and **5k** are, respectively, 8.9 and -2.0 kcal mol<sup>-1</sup>. This large difference is due to the fact that in **5k** there is a vacant coordination site, whereas in **5j** the coordination site is occupied by the OH group. If we calculate these values relative to the **5**-MeCN + MA asymptote, the corresponding Gibbs reaction energies are 10.9 (**5j**) and 12.3 (**5k**) kcal mol<sup>-1</sup>. These  $\eta^1$ -O complexes rearrange to the  $\eta^2$ -CC complexes **6j** and **6k**. The Gibbs activation energies reported in Table 5 correspond to this rearrangement transition states and have been referred to **5** + MA.

The reaction proceeds with the insertion of the alkene in the Pd–Ph bond, leading to the formation of **7**. This process involves the formation of a CC bond between the phenyl group and the nonsubstituted carbon atom of the alkene ligand. The formation of the bond involving the substituted carbon atom of the alkene has not been considered, since it involves a very large energy barrier.<sup>15</sup>

This step is notably more favorable for **6j** than for **6k**, both kinetically and thermodynamically, due to the hydrogen bond interaction between the OH group of the pyridylpyrazole ligand in **6j** and the carbonyl group of the ester.

The complex **7** is stabilized through an interaction between Pd and the phenyl group. A conformational rearrangement leads to **7'**, stabilized through a C–H agostic interaction. This step is the one that determines which is the geometric isomer of the

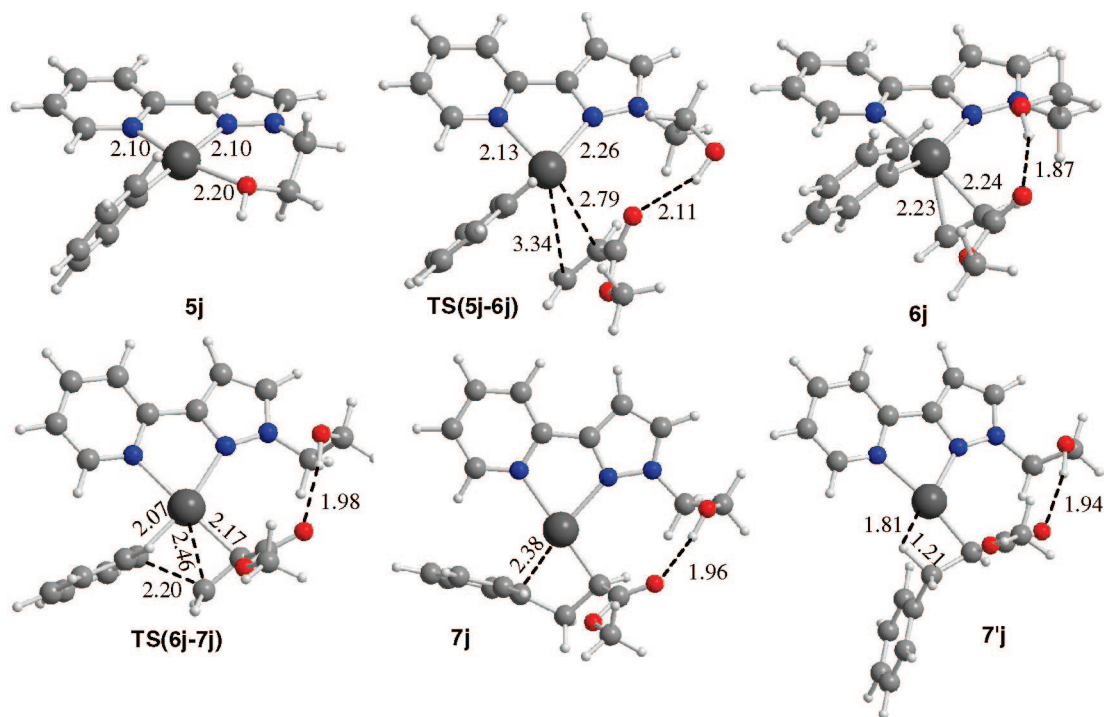


**Figure 5.** Structure of stationary points corresponding to reaction between **5j** and methyl acrylate. Selected interatomic distances are in Å.

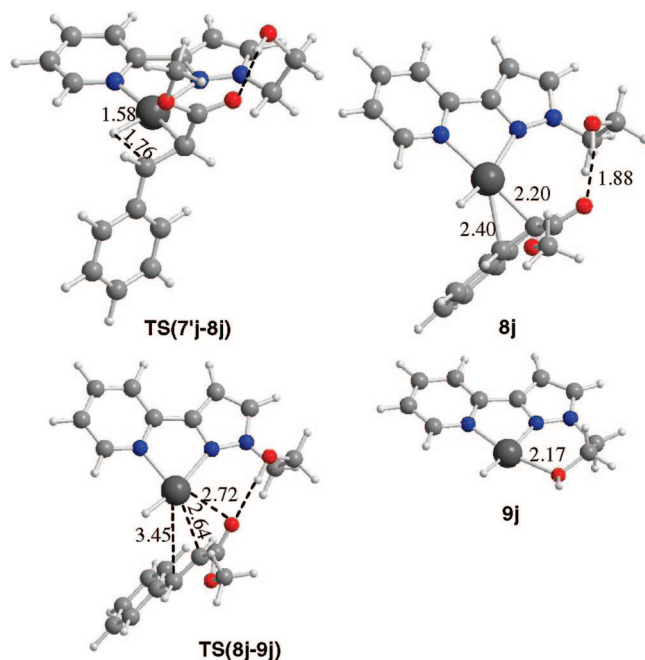


**Figure 6.** Structures of stationary points corresponding to  $\beta$ -hydride elimination from **7j**. Selected interatomic distances are in Å.

final product to be formed. In **7'j** the dihedral angle around the C(Ph)–C(CO<sub>2</sub>Me) bond is  $-141.6^\circ$ . There is an alternative conformer, **7''j**, with a dihedral angle of  $-19.6^\circ$ , which would lead to the *Z* isomer of methyl cinnamate, but it is 5.0 kcal mol<sup>-1</sup> higher in energy than **7'j** at the B3LYP/LANL2DZ(d) level.

The next step is a  $\beta$ -hydride elimination, which leads to the formation of the (alkene)(hydride)Pd cation **8**. The reaction proceeds with the dissociation of the methyl cinnamate ligand and the formation of **9**, which bears a vacant coordination site

**Table 6.** Gibbs Reaction Energies<sup>a</sup> for the Proton Transfer between **9** and Trimethylamine

	<b>9k</b>	<b>9j</b>
<b>9</b> + NMe <sub>3</sub> → <b>9</b> -NMe <sub>3</sub>	16.8	17.0
<b>9</b> -NMe <sub>3</sub> → <b>3</b> -HNMe <sub>3</sub> <sup>+</sup>	6.2	-2.3
<b>3</b> -HNMe <sub>3</sub> <sup>+</sup> → <b>3</b> + HNMe <sub>3</sub> <sup>+</sup>	-8.0	-0.4

<sup>a</sup> In acetonitrile solution at 298.15 K and 1 mol L<sup>-1</sup>. All values in kcal mol<sup>-1</sup>.

on Pd. In **9j** this vacant coordination site is occupied by the OH of the hydroxyethyl group.

The dissociation of methyl cinnamate (MC) takes place in two steps. The first one is a  $\eta^2$ -CC/ $\eta^1$ -O rearrangement, which involves a transition state, and the second one is the decoordination of methyl cinnamate. The Gibbs activation energies shown in Table 3 correspond to these rearrangement transition states. The Gibbs reaction energies for the dissociation of the  $\eta^1$ -O complexes are  $-11.4$  (**8j**) and  $0.8$  (**8k**) kcal mol<sup>-1</sup>.

The last part of the catalytic cycle involves a proton transfer between **9** and the base. We have studied this process using triethylamine and trimethylamine as bases.

For trimethylamine we have done a more detailed study of the potential energy surface, and the results are summarized in Table 6 and Figure 7.

The interaction between **9j** or **9k** and trimethylamine leads to the formation of a hydrogen bond complex, which is stable in the gas phase, but becomes unfavored in solution. Then the proton is transferred, leading to the formation of a **3**-HNMe<sub>3</sub><sup>+</sup> complex. For **9k** the potential energy surface for such a process is very flat, and it has not been possible to locate a transition state. On the other hand, for **9j** we have located the transition state, and the computed Gibbs activation energy is 8.1 kcal mol<sup>-1</sup>.

The complete Gibbs energy profiles for both reactions are shown in Figure 8. For the Pd–I dissociation step we have considered the participation of a acetonitrile molecule for both

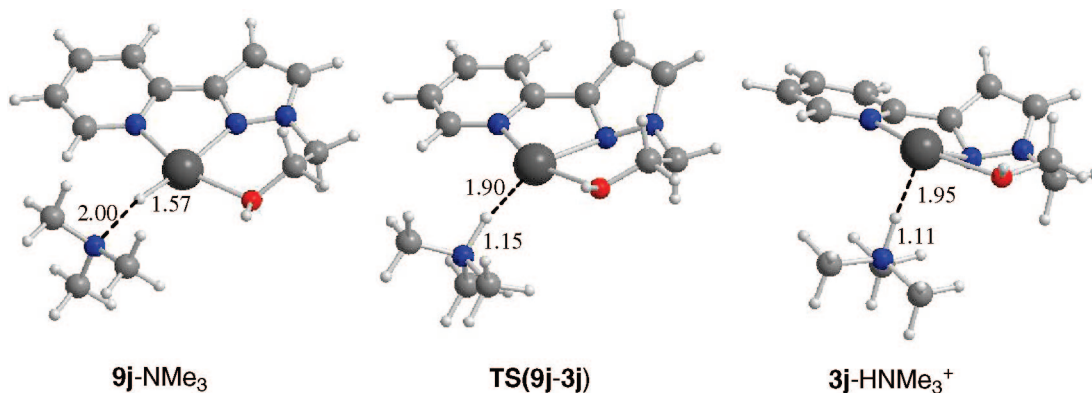


**Figure 7.** Structures of stationary points corresponding to proton transfer between **9j** and trimethylamine. Selected interatomic distances are in Å.

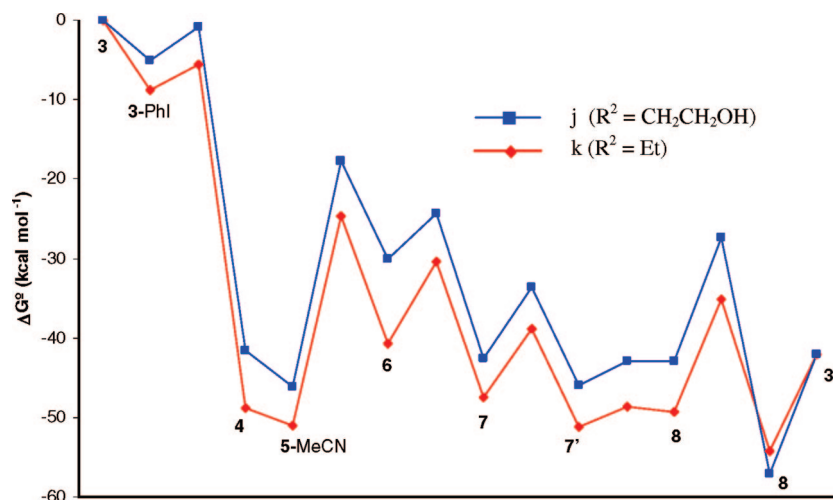


**Figure 8.** Gibbs energy profiles for the catalytic cycle corresponding to the reaction between phenyl iodide and methyl acrylate catalyzed by **3j** (in blue) and **3k** (in red) in acetonitrile solution.

**4j** and **4k**. As we can observe, the profile corresponding to  $R^2 = \text{Et}$  generally lies below the one corresponding to  $R^2 = \text{hydroxyethyl}$ . Experiments indicate that the complexes bearing a ligand with a hydroxyethyl group are more efficient than those with an ethyl group (see Table 1). The origin of this different behavior may be in the Pd–I dissociation step. As we have seen, the dissociation is much more favorable for **4j** than for **4k**, in such a way that the process is favored even in the absence of a coordinating solvent molecule. On the other hand, for **4k** the Pd–I dissociation would be in competition with the dissociation of the Pd–N(pyrazole) bond. Another effect of the hydroxyethyl ligand is its ability to form hydrogen bonds with the coordinated ester. This is especially evident in the olefin insertion step ( $6 \rightarrow 7$ ), which is more favorable both kinetically and thermodynamically for **6j** than for **6k** (see Table 3).

## Conclusions

Pd complexes with pyridylpyrazole ligands have been shown to be active as catalysts in the Heck reaction between phenyl halides and *tert*-butyl acrylate. The most efficient catalysts are the ones in which the pyrazole ring has a hydroxyethyl substituent at N1. The presence of an OH group in  $R^2$  favors the Pd–X dissociation, since it stabilizes the resulting cationic complex. In this way, the dissociation is thermodynamically favorable even in the absence of a coordinating solvent molecule.

## Experimental Section

**General Methods.** Standard Schlenk techniques were employed throughout the synthesis using a double-manifold vacuum line with high-purity dry nitrogen. All reagents were commercial grade materials and were used without further purification. All solvents were dried and distilled by standard methods. The elemental analyses (C, H, N) were carried out by the staff of the Chemical Analyses Service of the Universitat Autònoma de Barcelona on a Carlo Erba CHNS EA-1108 instrument. Conductivity measurements were performed at room temperature (rt) in  $10^{-3}$  M acetone employing a Crison micro CM 2200 conductimeter. Infrared spectra were run on a Perkin-Elmer FT spectrophotometer series 2000  $\text{cm}^{-1}$  as NaCl, KBr pellets, or polyethylene films in the range 4000–100  $\text{cm}^{-1}$  under a nitrogen atmosphere. The  $^1\text{H}$  NMR,  $^{13}\text{C}\{^1\text{H}\}$  NMR, HMQC, and NOESY spectra were run on a NMR-FT Bruker 250 MHz instrument.  $^1\text{H}$  NMR and  $^{13}\text{C}\{^1\text{H}\}$  NMR chemical shifts ( $\delta$ ) were determined relative to internal TMS and are given in ppm. Electronic impact mass spectra were measured on a Hewlett-Packard HP-5989.

The pyridylpyrazole ligands **1b–1i** and the Pd(II) complexes **2b–2i** were prepared according to the methods described in the literature.<sup>25,27,29,31,34</sup>

Samples of  $[\text{PdCl}_2(\text{CH}_3\text{CN})_2]^{35}$  were prepared as described in the literature. The reaction progress was analyzed by GLC

(34) Perez, J. A. Thesis, 2003.

(35) *Synthesis of Organometallic Compounds: a Practice Guide*; Komiya, S., Ed.; Wiley: New York, 1997.

(HP5480), and the % conversion was measured relative to internal standard decane.

**Synthesis of Complex 2a.** The ligand **1a** (0.40 mmol; 0.10 g) dissolved in dry acetonitrile (20 mL) was added to a solution of  $[\text{PdCl}_2(\text{CH}_3\text{CN})_2]$  (0.40 mmol; 0.10 g) in dry acetonitrile (20 mL). The resulting solution was stirred at room temperature for 12 h. The solution was concentrated until an orange crystalline precipitate appeared. The solid was filtered off, washed with diethyl ether (5 mL), and dried under vacuum.

**2a:** Yield: 70%.  $\text{C}_{16}\text{H}_{15}\text{N}_3\text{OCl}_2\text{Pd}$  (465.64). Anal. Calc: C, 43.44, H, 3.39, N, 9.50. Found: C, 43.22, H, 3.28, N, 9.37. Conductivity ( $\Omega^{-1} \text{cm}^2 \text{mol}^{-1}$ ,  $9.8 \times 10^{-4} \text{ M}$  in DMSO): 25.6. IR: (KBr,  $\text{cm}^{-1}$ ) 3475  $\nu(\text{O-H})$ , 3105  $\nu(\text{C-H})_{\text{ar}}$ , 2924  $\nu(\text{C-H})_{\text{al}}$ , 1615  $\nu(\text{C}=\text{C})$ ,  $\nu(\text{C}=\text{N})_{\text{ar}}$ , 1465, 1444  $\delta(\text{C}=\text{C})$ ,  $\delta(\text{C}=\text{N})_{\text{ar}}$ , 781, 701  $\delta(\text{C-H})_{\text{oop}}$ ; (polyethylene,  $\text{cm}^{-1}$ ): 462  $\nu(\text{Pd-N})$ , 345, 327  $\nu(\text{Pd-Cl})$ .  $^1\text{H}$  NMR (DMSO solution, 250 MHz)  $\delta$ : 9.01 (1H, d,  $^3J = 5.9 \text{ Hz}$ ,  $H_8$ ), 8.30 (1H, t,  $^3J = 7.4 \text{ Hz}$ ,  $H_{10}$ ), 8.22 (1H, d,  $^3J = 6.4 \text{ Hz}$ ,  $H_{11}$ ), 7.69–7.65 (6H, m,  $H_9$ ,  $H_{\text{Ph}}$ ), 7.49 (1H, s,  $H_4$ ), 4.85 (2H, t,  $^3J = 5.2 \text{ Hz}$ , pz- $\text{CH}_2\text{-CH}_2\text{-OH}$ ), 4.73 (1H, t,  $^3J = 4.8 \text{ Hz}$ , OH), 3.79 (2H, dd,  $^3J = 5.2 \text{ Hz}$ ,  $^3J = 4.8 \text{ Hz}$  pz- $\text{CH}_2\text{-CH}_2\text{-OH}$ ) ppm.  $^{13}\text{C}\{^1\text{H}\}$  NMR (DMSO solution, 63 MHz)  $\delta$ : 152.2 ( $C_3$ ), 151.3 ( $C_6$ ), 149.1 ( $C_8$ ), 148.6 ( $C_5$ ) 141.1 ( $C_{10}$ ), 130.8 ( $C_{12}$ ), 129.7 ( $C_{15}$ ), 129.4 ( $C_{13}$ ,  $C_{17}$ ), 128.7 ( $C_{14}$ ,  $C_{16}$ ), 124.9 ( $C_9$ ), 122.2 ( $C_{11}$ ), 105.5 ( $C_4$ ), 60.3 (pz- $\text{CH}_2\text{-CH}_2\text{-OH}$ ), 51.2 (pz- $\text{CH}_2\text{-CH}_2\text{-OH}$ ) ppm.

#### General Procedure for the Heck-Type Coupling Reactions.

Prescribed amount of catalyst, base (1.4 equiv), alkene (1.5 equiv), aryl halide (1.0 equiv), and decane were placed in a round-bottom flask. Solvent (2 mL) was added, and the mixture was heated to the prescribed temperature until reaction completion.

**Computational Details.** The molecular geometries have been fully optimized through density functional calculations using the B3LYP functional.<sup>36</sup> The LANL2DZ basis set has been used for Pd, Cl, Br, and I. This basis set included effective core potentials for the inner shells (up to 3p for Pd) and a double- $\zeta$  basis set for the valence shells.<sup>37</sup> For the remaining atoms the D95V basis set has been used.<sup>38</sup> A set of 3d polarization functions has been included for all atoms except Pd and H.<sup>39</sup> This basis set will be named as LANL2DZ(d). Harmonic vibrational frequencies have

been computed at this level of calculation for all structures to characterize them as energy minima (all frequencies are real) or transition states (one and only one imaginary frequency). The solvent effect has been included through the CPCM method<sup>40</sup> using acetonitrile ( $\epsilon = 36.64$ ) as solvent. In these calculations a set of diffuse sp functions has been included in all atoms except H and Pd.<sup>41</sup> All these calculations have been done using the Gaussian-03 program.<sup>42</sup> Finally, the energies of all structures have been recomputed with the ADF program<sup>43</sup> at the B3LYP<sup>36,44</sup> level of calculation using an all-electron TZ2P basis set. Relativistic effects have been included using the ZORA method.<sup>44</sup> Gibbs energies in solution were computed from energies computed with the TZ2P basis set, zero-point and thermal corrections to the energy and entropies computed with the LANL2DZ(d) basis set, and solvation energies computed with the CPCM method. The reference state for the reported Gibbs energies in solution is 298.15 K and 1 mol  $\text{L}^{-1}$ .

**Acknowledgment.** Support by the Spanish Ministerio de Educación y Cultura (Projects CTQ2007-63913/BQU and CTQ2004-01067/BQU) and access to the computational facilities of Centre de Supercomputació de Catalunya (CESCA) are gratefully acknowledged.

**Supporting Information Available:** X-ray data (CIF) and crystallographic description of complex **2a**, and energies and Cartesian coordinates of all calculated structures. This material is available free of charge via the Internet at <http://pubs.acs.org>.

OM7009182

(40) (a) Klamt, A.; Schüürmann, G. *J. Chem. Soc., Perkin Trans.* **1993**, 2, 799. (b) Barone, V.; Cossi, M. *J. Phys. Chem. A* **1998**, *102*, 1995. (c) Cossi, Rega, N.; Scalmani, G.; Barone, V. *J. Comput. Chem.* **2003**, *24*, 669.

(41) Standard exponents were used for C (0.0438), N (0.0639), O (0.0845), Cl (0.0483), and Br (0.035). The exponent for I (0.0368) was optimized for the atomic ground-state anion by Ted Packwood at NDSU. Diffuse functions for this and other heteroatoms may be found at the Web site: <http://www.msg.ameslab.gov/games/documentatation.html>.

(42) Frisch, M. J.; et al. *Gaussian 03*, Revision C.02; Gaussian, Inc.: Wallingford, CT, 2004, <http://www.gaussian.com>.

(43) (a) te Velde, T. G.; Bickelhaupt, F. M.; Baerends, E. J.; Fonseca Guerra, C.; van Gisbergen, S. J. A.; Snijders, J. G.; Ziegler, T. *J. Comput. Chem.* **2001**, *22*, 931. (b) *ADF200501*, SCM, Theoretical Chemistry, Vrije Universiteit: Amsterdam, The Netherlands, <http://www.scm.com>.

(44) Watson, M. A.; Handy, N. C.; Cohen, A. J. *J. Chem. Phys.* **2003**, *119*, 6475.

(45) (a) van Lenthe, E.; Baerends, E. J.; Snijders, J. G. *J. Chem. Phys.* **1993**, *99*, 4597. (b) van Lenthe, E.; Baerends, E. J.; Snijders, J. G. *J. Chem. Phys.* **1994**, *101*, 9783. (c) van Lenthe, E.; Snijders, J. G.; Baerends, E. J. *J. Chem. Phys.* **1996**, *105*, 6505. (d) van Lenthe, E.; van Leeuwen, R.; Baerends, E. J.; Snijders, J. G. *Int. J. Quantum Chem.* **1996**, *57*, 281. van Lenthe, E.; Ehlers, A. E.; Baerends, E. J. *J. Chem. Phys.* **1999**, *110*, 8943.

(36) (a) Becke, A. D. *J. Chem. Phys.* **1993**, *98*, 5648. (b) Lee, C.; Yang, W.; Parr, R. G. *Phys. Rev. B* **1988**, *37*, 785. (c) Stephens, P. J.; Devlin, F. J.; Chabalowski, C. F.; Frisch, M. J. *J. Phys. Chem.* **1994**, *98*, 11623.

(37) (a) Hay, P. J.; Wadt, W. R. *J. Chem. Phys.* **1985**, *82*, 270. (b) Wadt, W. R.; Hay, P. J. *J. Chem. Phys.* **1985**, *82*, 284.

(38) Dunning, T. H.; Hay, P. J. In *Modern Theoretical Chemistry*, Vol. 3; Schaeffer, H. F., III, Ed.; Plenum: New York, 1976; p 1.

(39) Standard exponents were used for C (0.75), N (0.80), O (0.85), Cl (0.60), and Br (0.338). The exponent for I (0.266) has been taken from: Huzinaga, S.; Andzelm, J.; Klobukowski, M.; Radzio-Andzelm, E.; Sakai, Y.; Tatemaki, H. *Gaussian Basis Sets for Molecular Calculations*; Elsevier: Amsterdam, 1984.